

PREDICTION OF TEMPERATURE AND CONCENTRATION DISTRIBUTIONS OF DISTILLATION SIEVE TRAYS BY CFD

Rahbar Rahimi, Mahmood-Reza Rahimi, Farhad Shahraki, Morteza Zivdar
Department of Chemical Engineering, Sistan and Baluchistan University, Zahedan,
98164, Iran; E-mail: rahimi@hamoon.usb.ac.ir

A 3-D two-fluid CFD model was developed to predict temperature and concentration distributions on sieve trays of distillation columns. The gas phase is dispersed and the liquid phase is continuous are modeled in the Eulerian framework as two interpenetrating phases with interphase momentum, heat and mass transfer. The computational domain is considered to be equal to tray spacing. The tray geometries are based on the large rectangular tray of Dribika and Biddulph (AIChE. J., 32, 1864, 1986). In this work a CFD simulation is developed to predict the hydraulic behavior and concentration and temperature distributions of distillation sieve trays. In this study the main objective has been to find the extent to which CFD can be used as a prediction tool for real behavior, concentration and temperature distributions and also design of sieve trays. The simulation results are shown that CFD is a powerful tool in tray design, analysis and trouble shooting, and can be considered as a new approach for efficiency calculations.

KEYWORDS: computational fluid dynamics, concentration distribution, distillation column, sieve tray, temperature distribution

INTRODUCTION

Distillation is a separation process of major importance in the chemical industries, and known as the energy intensive process. Distillation involves simultaneous mass and heat transfer between the liquid and vapor phases. A good understanding of heat and mass transfer and pressure drop fundamentals across a tray will enable the column designer effectively determine the optimal equipment design.

In this work a CFD simulation is developed to give the predictions of the fluid flow patterns, and heat and mass transfer of distillation sieve trays. The main objective has been to find the extent to which CFD can be used as a design and prediction tool for real behavior, concentration and temperature distributions, and efficiencies of industrial trays, whilst appreciating works of pioneers [1,2,3,4,5].

Therefore, CFD predictions of temperature and concentration profiles were compared with the experimental data of Dribika and Biddulph [8]. The simulation results are shown that CFD can be used as a powerful tool in tray design and analysis, and can be considered as a new approach for efficiency calculations [12].

MODEL EQUATIONS

The dispersed gas and the continuous liquid are modeled in the Eulerian frame work as two interpenetrating phases having separate transport equations.

The two-fluid conservation equations for adiabatic two-phase flow are as follows:

Continuity equations

Gas phase:

$$\frac{\partial}{\partial t}(r_G \rho_G) + \nabla \cdot (r_G \rho_G \mathbf{V}_G) + S_{LG} = 0 \quad (1)$$

Liquid phase:

$$\frac{\partial}{\partial t}(r_L \rho_L) + \nabla \cdot (r_L \rho_L \mathbf{V}_L) - S_{LG} = 0 \quad (2)$$

S_{LG} is the rate of mass transfer from liquid phase to the Gas phase and vice versa. Mass transfer between phases must satisfy the local balance condition:

$$S_{LG} = -S_{GL} \quad (3)$$

Momentum conservation

Gas phase:

$$\begin{aligned} & \frac{\partial}{\partial t}(r_G \rho_G \mathbf{V}_G) + \nabla \cdot (r_G (\rho_G \mathbf{V}_G \mathbf{V}_G)) \\ & = -r_G \nabla P_G + \nabla \cdot (r_G \mu_{\text{eff,G}} (\nabla \mathbf{V}_G + (\nabla \mathbf{V}_G)^T)) + r_G \rho_G \mathbf{g} - \mathbf{M}_{GL} \end{aligned} \quad (4)$$

Liquid phase:

$$\begin{aligned} & \frac{\partial}{\partial t}(r_L \rho_L \mathbf{V}_L) + \nabla \cdot (r_L (\rho_L \mathbf{V}_L \mathbf{V}_L)) \\ & = -r_L \nabla P_L + \nabla \cdot (r_L \mu_{\text{eff,L}} (\nabla \mathbf{V}_L + (\nabla \mathbf{V}_L)^T)) + r_L \rho_L \mathbf{g} + \mathbf{M}_{GL} \end{aligned} \quad (5)$$

\mathbf{M}_{GL} describes the interfacial forces acting on each phase due to the presence of other phase.

Volume conservation equation

This is simply the constraint that the volume fractions sum to unity:

$$r_L + r_G = 1 \quad (6)$$

Pressure constraint

The complete set of hydrodynamic equations represent 9 ($4N_p + 1$) equations in the 10 ($5N_p$) unknowns U_L , \mathbf{V}_L , W_L , r_L , P_L , U_G , \mathbf{V}_G , W_G , r_G , P_G . We need one ($N_p - 1$) more equation to close the system. This is given by constraint on the pressure, namely that

two phases share the same pressure field:

$$P_L = P_G = P$$

Energy conservation

Gas phase:

$$\frac{\partial}{\partial t}(r_G \rho_G h_G) + \nabla \cdot (r_G \rho_G \mathbf{V}_G h_G) = -\nabla \cdot \mathbf{q} + (Q_{LG} + S_{LG} h_{LG}) \quad (7)$$

Liquid phase:

$$\frac{\partial}{\partial t}(r_L \rho_L h_L) + \nabla \cdot (r_L \rho_L \mathbf{V}_L h_L) = -\nabla \cdot \mathbf{q} - (Q_{LG} + S_{LG} h_{LG}) \quad (8)$$

h_L and h_G are specific enthalpies of phase L and G, respectively. The first term in the parentheses on the right hand side of above equations is the energy transfer between phases, and the second term is the energy transfer associated with the mass transfer between phases. Heat transfer between phases must satisfy the local balance condition:

$$Q_{LG} = -Q_{GL} \quad (9)$$

Mass-Transfer equations

Transport equations for mass fraction of light component A can be written

Gas phase:

$$\frac{\partial}{\partial t}(r_G \rho_G Y_A) + \nabla \cdot [r_G (\rho_G \mathbf{V}_G Y_A - \rho_G D_{AG} (\nabla Y_A))] - S_{LG} = 0 \quad (10)$$

Liquid phase:

$$\frac{\partial}{\partial t}(r_L \rho_L X_A) + \nabla \cdot [r_L (\rho_L \mathbf{V}_L X_A - \rho_L D_{AL} (\nabla X_A))] + S_{LG} = 0 \quad (11)$$

Closure models

The closure models are required for interphase transfer quantities, momentum, heat and mass transfer, and turbulent viscosities.

The turbulence viscosities were related to the mean flow variables by using the standard $k - \varepsilon$ model.

The rate of energy transfer between phases can be written:

$$Q_{LG} = \beta_{LG} a_c (T_L - T_G) \quad (12)$$

β_{LG} represents heat transfer coefficient between phases. An appropriate value of heat transfer coefficient can be obtained by using suitable correlations of Nusselt number.

In the absence of sufficient reliable data, the effect of other transport phenomena on the momentum transfer (coupling) was neglected.

The interphase momentum transfer term \mathbf{M}_{GL} is basically interphase drag force per unit volume. With the gas as the disperse phase, the equation for \mathbf{M}_{GL} is

$$\mathbf{M}_{GL} = \frac{3 C_D}{4 d_G} r_G \rho_L |\mathbf{V}_G - \mathbf{V}_L| (\mathbf{V}_G - \mathbf{V}_L) \quad (13)$$

C_D is drag coefficient. Its value for the case of distillation is not well known. A constant value of 0.44 is appropriate for large bubbles of spherical cap shape. However, for the froth flow regime, which is dominant region in distillation, it is not applicable. Further, the bubbles are from 10–20 mm in diameter with bubble rise velocity of 1.5 m/s, to 2–5 mm in diameter, with rise velocity of about 0.25 m/s [8]. Therefore any equation for C_D that is independent of bubble diameter seems most appropriate.

Krishna et al., [9] have used an equation for drag term that was developed from their studies on the bubble column. It was combined with Bennett et al relationship for gas holdup to eliminate the bubble diameter. This led to equation (14) which is independent of bubble diameter and is useful for prediction of tray hydraulics by use of CFD.

$$\mathbf{M}_{GL} = \frac{(\bar{r}_G)^2}{(1.0 - \bar{r}_G) V_s^2} g(\rho_L - \rho_G) r_G r_L |\mathbf{V}_G - \mathbf{V}_L| (\mathbf{V}_G - \mathbf{V}_L) \quad (14)$$

The mass-transfer rate can be calculated by equation.

$$S_{LG} = K_{OG} a_e M_A (y_A - y_A^*) = K_{OL} a_e M_A (x_A^* - x_A) \quad (15)$$

Where $K_{OG} = 1/(1/k_G + m/k_L)$, $K_{OL} = 1/(1/mk_G + 1/k_L)$ and $y_A^* = mx_A$ is the vapor composition in equilibrium with x_A . The local mass-transfer rate S_{LG} is calculated by above equations. The value of m was determined by the equilibrium data of Dribika and Biddulph [8].

The local liquid and gas mass transfer coefficients, using penetration theory, are given by equations 16 and 17, respectively.

$$k_L = 2 \sqrt{\frac{D_{AL}}{\pi \theta_L}} \quad (16)$$

$$k_G = 2 \sqrt{\frac{D_{AG}}{\pi \theta_G}} \quad (17)$$

D_{AL} and D_{AG} are diffusion coefficients in liquid and gas phases, respectively. The contact time for vapor in the froth region θ_G is defined as $\theta_G = d_G/V_P$, where V_P is velocity of

vapor through the tray perforations. The contact time for liquid, θ_L , is d_G/V_R , where average rise velocity, V_R , of bubbles through the froth is given by:

$$V_R = \frac{V_B}{(1 - \bar{r}_L)} = \frac{V_P \left(\frac{A_P}{A_B} \right)}{(1 - \bar{r}_L)} \quad (18)$$

A_P/A_B is perforated area to total bubbling area ratio.

Taylor and Krishna [8] mentioned that only 10% of mass transfer occurs by bubbles of small size, whilst 90% of mass transfer is due to bubbles of large size. Hence, in one approach the characteristic length, d_G , may be assumed to be equal to mean diameter of bubbles. This is assumed to be 5 mm for $F_s = 0.4$. The effective vapor-liquid interfacial area can be determined directly from the liquid holdup and the mean bubble diameter by the following equation:

$$a_e = \frac{6(1 - \bar{r}_L)}{d_G} \quad (19)$$

It is known that closure models have important effects on the accuracy of final results of a CFD simulation. Therefore, their determination is the most important part in each CFD simulation. But, unfortunately in the case of sieve tray, these models are not presented or not tested for CFD application. Therefore further improvement and refinement of the required closure models, if more refined experimental data on flow and concentration distributions become available can be subject of future investigations.

FLOW GEOMETRIES

In this work at first the proposed simulation was used to the Dribika and Biddulph [7] large rectangular sieve tray, for determination of hydraulic parameters, temperature, and concentration profiles. The simulation results were then compared against the experimental data of Dribika and Biddulph [7].

The experimental rig of Dribika and Biddulph [7] consisted of three rectangular distillation trays having dimensions of 1067×89 mm, which the middle one being the test-tray. The test-tray was designed with six equally spaced points for sampling and temperature measurement along the centerline where mentioned by points "S" in Figure 1, details of the tray are given in Table 1. The column was operated at total reflux and

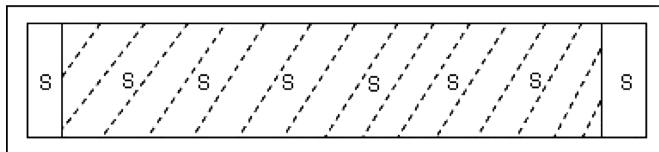


Figure 1. Details of rectangular tray showing sample/temperature points [11]

Table 1. Rectangular tray specifications

Weir length	83 mm	Hole diameter	1.8 mm
Outlet weir height	25 mm	Tray spacing	154 mm
Inlet weir height	4.8 mm	Liquid flow path	991 mm
Percentage free area	8%		

atmospheric pressure, and carried out at a vapor phase F_g factor of $0.4 \text{ m/s (kg/m}^3)^{1/2}$ and covered a wide range of composition. The system used was methanol–*n*-propanol and ethanol–*n*-propanol. All the hot surfaces of the equipment were insulated with 50 mm thick glass fiber material and aluminum cladding, therefore, the column was adiabatic. Hence adiabatic form of CFD equations are applicable.

WALL AND BOUNDARY CONDITIONS

In this steady state simulation, the following boundary conditions are specified. A uniform liquid inlet velocity, temperature, and concentration profiles are used and liquid is considered as a pure phase, means that only liquid enters through the down comer clearance. This is a good approximation for rectangular tray, because at this F_g factor (0.4) the entrainment was found to be less than 0.02 and this value would have negligible effect on the flow rates [7]. In addition negligible weeping was observed by the investigators.

The gas volume fraction at the inlet holes was specified to be unity. The liquid- and vapor-outlet boundaries were specified as mass flow boundaries with fractional mass flux specifications. At the liquid outlet, only liquid was assumed to leave the flow geometry and only gas was assumed to exit through the vapor outlet. These specifications are in agreement with the specifications at the gas inlet and liquid inlet, where only one fluid was assumed to enter.

A no-slip wall boundary condition was specified for the liquid phase and a free slip wall boundary condition was used for the gas phase. The flow conditions at the outlet weir are considered as fully developed in velocity, temperature and concentration. The normal direction gradients of temperature and concentration at the walls are zero.

SIMULATION RESULTS AND DISCUSSION

Most of simulations were conducted using dual processor machines ($2 \times 2.4 \text{ GHz}$) run in parallel. CFD analysis was carried out using 5.7 of Ansys, Inc [11]. Simulations were conducted with CPU times per CFD simulations, for convergence, varying from as low as 16 h to about 3 weeks.

HYDRODYNAMICS

Van Batten and Krishna [4,5,9] and Gesit et al. [1] found that CFD give clear liquid height values larger than the experimental ones. This is mainly due to over prediction of gas holdup by Benett et al. [10] equation that incorporates in equation 17. The over prediction

we have encountered are about 4%. This is clear from Figures 2(a) and (b). Figure 2(c) is a contour of liquid holdup of for $F_s = 0.4$. Variation of froth height is also shown by Figures 3(a) and (b). More results are presented by R. Rahimi et al. in CET [12].

Dribika and Biddulph [7] have presented the liquid concentration and temperature profiles at various compositions at $F_s = 0.4$ and total reflux condition. The simulation results were compared against their experimental data.

The tray length was divided into 6 equal sections. The mean liquid concentration for each section was determined by integration.

In Figure 4 the predicted composition profiles using the CFD model, for MeOH/nPrOH and EtOH/nPrOH pairs, were compared against experimental data of Dribika and Biddulph [7]. The obtained results are in close agreement with experimental data, and the trend of CFD results is exactly correct. Since the column was operated at total reflux conditions, the vapor compositions is related to the liquid compositions according to equation $y_{n+1} = x_n$, the CFD results are generally in good agreement with this equation. The mean average error is about 0.5% that may be due to truncation errors and uncertainties in closure models used in these simulations.

LIQUID TEMPERATURE PROFILES

The predicted liquid temperature profiles, for MeOH/nPrOH and EtOH/nPrOH systems, respectively, are shown in Figure 5 compared with experimental data of Dribika and

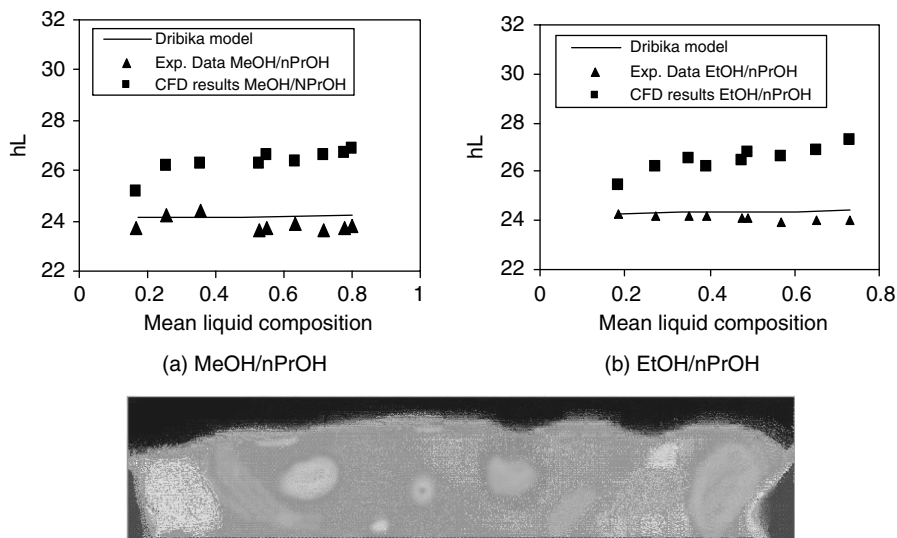


Figure 2. Variation of liquid holdup with mean liquid composition $F_s = 0.4$

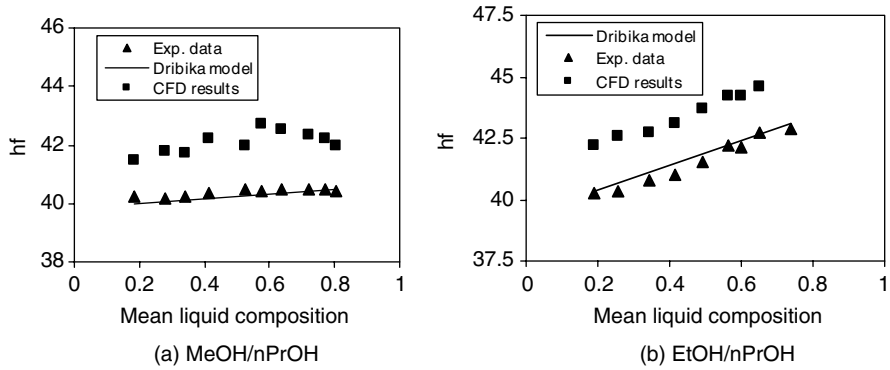


Figure 3. Variation of froth height with mean liquid composition, rectangular tray, $F_s = 0.4$, Compositions profiles

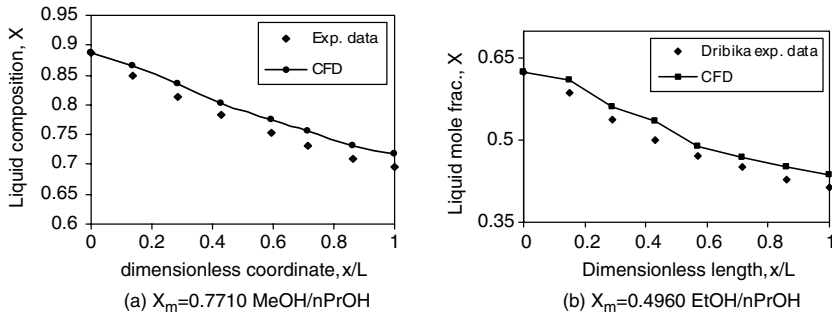


Figure 4. Center-line liquid composition profiles for rectangular tray, binary system

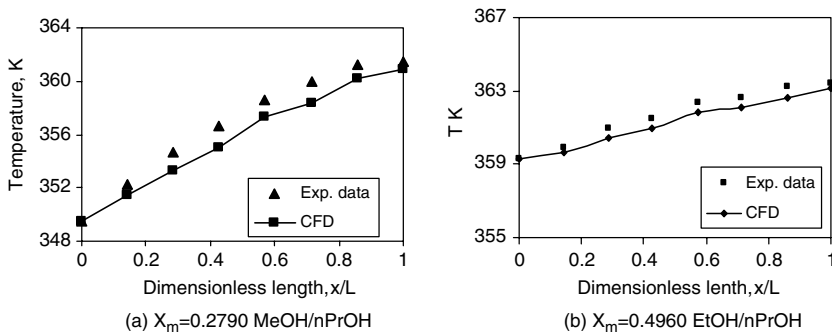


Figure 5. Center-line temperature profiles for rectangular tray, binary system

Biddulph [7]. The predictions are generally in very close agreement with experimental data. Mean temperature in each cell is calculated by integration. The results confirm that at the condition of Dribika and Biddulph [7] experiments the mixed liquid flow in the transverse direction is acceptable, but in large diameter trays the variation of liquid concentration in transverse direction may be important.

CONCLUSION

A 3-D two-fluid CFD model was developed in the Eulerian framework to predict the hydrodynamics, heat and mass transfer performance of sieve trays. The tray geometries and operating conditions are based on the experimental work of Dribika and Biddulph [8]. The hydraulics parameters, velocity, temperature and concentration distributions were determined. The results are in close agreement with experimental data.

Results of CFD model are dependent on the closure models. The future works can be focused on development and refinement of closure laws for interphase momentum heat and mass transfer and coupling between them, and development of required correlations based on bubble diameter.

NOMENCLATURE

- A_B = tray bubbling area, m^2
- A_H = total area of holes, m^2
- A_P = perforated area, m^2
- a_e = effective interfacial area per unit volume, m^{-1}
- C_D = drag coefficient
- d_G = mean bubble diameter, m
- D_{AG}, D_{AL} = diffusion coefficient of A in gas and liquid phases, m/s^2
- F_S = Flooding factor = $V_S \sqrt{\rho_G}$
- g = gravity acceleration, m/s^2
- h_G, h_L = specific enthalpy of gas and liquid kJ/kg
- $h_{LG} = (h_L - h_G)$
- k_G, k_L = gas and liquid phase mass transfer coefficients, m/s
- K_{oG}, K_{oL} = gas and liquid phase overall mass transfer coefficient, m/s
- M_{GL} = interphase momentum transfer, $kg \cdot m^{-2} \cdot s^{-2}$
- M_A = molecular weight of component A
- P = total pressure, Nm^{-2}
- P_G, P_L = gas and liquid phase pressure, $N \cdot m^{-2}$
- q = flux of enthalpy, w/m^2
- Q_L = liquid volumetric flow rate, m^3/s
- Q_{LG} = energy transfer between liquid and gas phases, w/m^3
- r_G, r_L = gas and liquid phase volume fraction, dimensionless
- \bar{r}_G = average gas holdup fraction in froth, dimensionless
- S_{LG} = rate of interphase mass transfer, kg/m^3s
- T = temperature, K

- U, V, W = x, y, z components of velocity, m/s
 V_G, V_L = gas and liquid phase velocity vector, m/s
 V_P = vapor velocity through the tray perforations, m/s
 V_R = bubble rise velocity, m/s
 V_S = gas phase superficial velocity based on bubbling area, m/s
 V_{slip} = slip velocity, m/s
 Y_A, X_A = mass fraction of A in gas and liquid phase
 x_A, y_A = mole fraction of A in liquid and gas phase
 x_A^*, y_A^* = equilibrium mole fractions
 x, y, z = coordination's, distance from origin, m

GREEK LETTERS

- $\mu_{eff,G}, \mu_{eff,L}$ = effective viscosity of gas and liquid, $kg \cdot m^{-1} \cdot s^{-1}$
 ρ_G, ρ_L = gas and liquid phase density, kg/m^3

REFERENCES

- Gesit, G. K., et al., "CFD Modeling of Flow Patterns and Hydraulics of Commercial-Scale Sieve Trays," *AICHE J.*, 49, 910 (2003).
- Mehta, B., K. T. Chuang, K. Nandakumar, "Model for Liquid Phase Flow on Sieve Trays," *Chem. Eng. Res. Des., Trans. Inst. Chem. Eng.*, 76, 843 (1998).
- Yu K. T., et al., "Computational Fluid Dynamics and Experimental Verification of Two Phase Two Dimensional Flow on a Sieve Column Tray" *Chem. Eng. Res. Des.* 77a, 554 (1999).
- Krishna, R., J. M. van Baten, J. Ellenberger, A. P. Higler, and R. Taylor, "CFD Simulations of sieve Tray Hydrodynamics," *Chem. Eng. Res. Des., Trans. Inst. Chem. Eng.*, 77, 639 (1999a).
- Van Baten, J. M., and R. Krishna, "Modeling Sieve Tray Hydraulics Using Computational Fluid Dynamics," *Chem. Eng. J.*, 77, 143 (2000).
- Wang X. L. et al. "Computational Fluid Dynamics Simulation of Three-Dimensional Liquid Flow and Mass Transfer on Distillation Column Trays" *Ind. Eng. Chem. Res.* 43, 2556–2567 (2004).
- Dribika, M. M., and M. W. Biddulph, "Scaling-up Distillation Efficiencies," *AICHE J.*, 32, 1864 (1986).
- Taylor R. R. Krishna, "Multicomponent Mass Transfer," John Wiley, New York (1993).
- Krishna, R., M. I. Urseau, J. M. Van Batten, and J. Ellenberger, "Rise Velocity of a Swarm of Large Gas Bubbles in Liquids," *Chem. Eng. Sci.*, 54,171 (1999b).
- Bennett, D. L., Agrawal, and P. J. Cook, "New Pressure Drop Correlation for Sieve Tray Distillation Column," *AICHE J.*, 29, 434 (1983).
- CFX User Manual, Ansys Inc., CFX 5.7: solver modeling.
- Rahimi, R., Rahimi, M. R., Sharaki, F., Zivdar, M., "Efficiency of Sieve Tray Distillation Columns by CFD Simulation", *Chem. Eng. Technol*, 29, 3 (2006).